J Mater Sci (2010) 45:719–724
DOI 10.1007/s10853-009-3990-x

Effect of initial microstructures on hot forging of Ca-containing cast Mg alloys

Masataka Hakamada · Kazunori Shimizu · Tomokazu Yamashita · Akira Watazu · Naobumi Saito · Hajime Iwasaki

Received: 10 June 2009 / Accepted: 20 October 2009 / Published online: 3 November 2009

Abstract Two cast noncombustible Mg–9Al–1Zn–1Ca alloys (composition in mass%) with coarse and fine initial microstructures were hot forged by compression at temperatures of 523–603 K and a true strain rate of 1–10^{-2} s^{-1}. The compressive stress–strain curves for the two alloys were similar and typical of metals undergoing dynamic recrystallization (DRX). The alloy with the coarse initial microstructure suffered from edge crack formation during hot forging, while the alloy with the fine initial microstructure exhibited smooth peripheral surfaces after hot forging at temperatures of 573 K and above. The reduction of grain size by DRX was similar in the two hot-forged alloys, but the recrystallized volume fraction was lower in the alloy with the coarse initial microstructure. Insoluble second phases (seemingly Al_2Ca) provide additional DRX sites, and thus it is expected that the finer initial cast microstructure will improve the microstructure in the resulting hot-forged Mg parts.

Introduction

The structural application of Mg alloys is now being attempted in various industries [1]; the high strength and low density of Mg alloys are appropriate for parts in automobiles, robots, and so forth. Mg alloy parts are mainly formed by die-casting; on the other hand, hot forging is another inexpensive technique of forming Mg alloys that achieves strengthening by grain refinement through dynamic recrystallization (DRX) [2–6].

In general, raw materials used for the hot forging of Mg alloys are extrusions because of their uniform and fine-grained microstructures [2]. However, recent progress in casting technology for Mg alloys may change this situation: that is, uniform and fine microstructures can be attained even in cast Mg alloys [7, 8]. Thus, as-cast and unextruded Mg alloys with uniform and fine microstructures may be used as raw materials for Mg alloy parts.

Ca is an element often added to Mg alloys to make them noncombustible [9]. The addition of Ca into molten Mg alloys greatly facilitates the casting operation without using a covering gas. When added to Mg, Ca generally forms hard second phases in the Mg matrix such as Mg_2Ca and Al_2Ca; however, under appropriate conditions, Ca-containing Mg alloys exhibit good workability in spite of the second phases [10–14]. Furthermore, the second phase particles appear to provide additional DRX sites, owing to both stress concentration and solute atom segregation around the particles [15–17], and contribute to homogeneous recrystallization in the hot-forged Mg alloy parts.

In this study, two cast Ca-containing Mg alloys with coarse and fine initial microstructures were hot forged by compression at elevated temperatures, and the effect of the initial cast microstructures on the hot forging was examined.

Experimental

Mg–9Al–1Zn–1Ca (composition in mass%) (AZX911) alloy was prepared by two casting methods: one was

M. Hakamada (✉) · A. Watazu · N. Saito
Materials Research Institute for Sustainable Development, National Institute of Advanced Industrial Science and Technology (AIST), Nagoya 463-8560, Japan
e-mail: masataka-hakamada@aist.go.jp

K. Shimizu · T. Yamashita
Magnesium Coordination Department, Sankyo Material, Inc., Takaoka 933-0838, Japan

H. Iwasaki
The Materials Process Technology Center, Tokyo 105-0011, Japan

typical direct chill billet casting and the other was adiabatic mold continuous casting, where a high cooling rate can be achieved because solidification in the adiabatic mold is inhibited. The microstructures of the as-cast AZX911 alloy samples prepared by the two casting methods are shown in Fig. 1. Both samples exhibited typical dendritic microstructures with insoluble second phases between the dendrite arms. The average grain size (measured by the linear intercept method [18]) and dendrite arm spacing obtained for each casting method are summarized in Table 1. Note that both the grain size and the dendrite arm spacing are smaller in the sample prepared by adiabatic mold continuous casting. Thus, the samples prepared by direct chill billet casting and adiabatic mold continuous casting are denoted as “coarse-microstructured” and “fine-microstructured” samples, respectively.

Cylindrical samples with a diameter of 10 mm and a height of 12 mm were mechanically cut from the half-radius positions of these as-cast billets for hot forging. Compression tests at 523, 573, and 603 K were conducted on the cylindrical samples with constant true strain rates of 1, 10^{-1}, and 10^{-2} s^{-1}, simulating the hot forging of the alloys. Boron nitride powder was sprayed on the surface of the samples for lubrication. The samples were water-quenched immediately after compression to a true compressive strain of 1.6. Microstructures at the midpoint of the hot-forged samples were observed using an optical microscope. The recrystallized grain size (d_{rec}) and recrystallized volume fraction (V_{rec}) were measured from the obtained micrographs. The former was measured using the linear intercept method [18] and the latter was estimated from the fractional area of the recrystallized region in the optical microscopic images. The features used to identify the recrystallized region were a small grain size and an equiaxed morphology [19].

Results and discussion

True compressive stress–strain (s–s) curves obtained from compression of the two samples at 573 K are shown in Fig. 2, under the assumption of uniform deformation. Both samples exhibited initial work hardening, stress peak at a strain of approximately 0.2, and then work softening and nearly constant stress at higher strains (although a slight increase in the flow stress, which is attributed to friction between the sample and compression plate, can be seen). This is likely to be due to DRX during the hot forging. The peak strain in the curves increased slightly with increasing strain rate. Flow stress was higher for compression with higher strain rates. The flow stresses in the coarse-microstructured samples were slightly lower than those in the

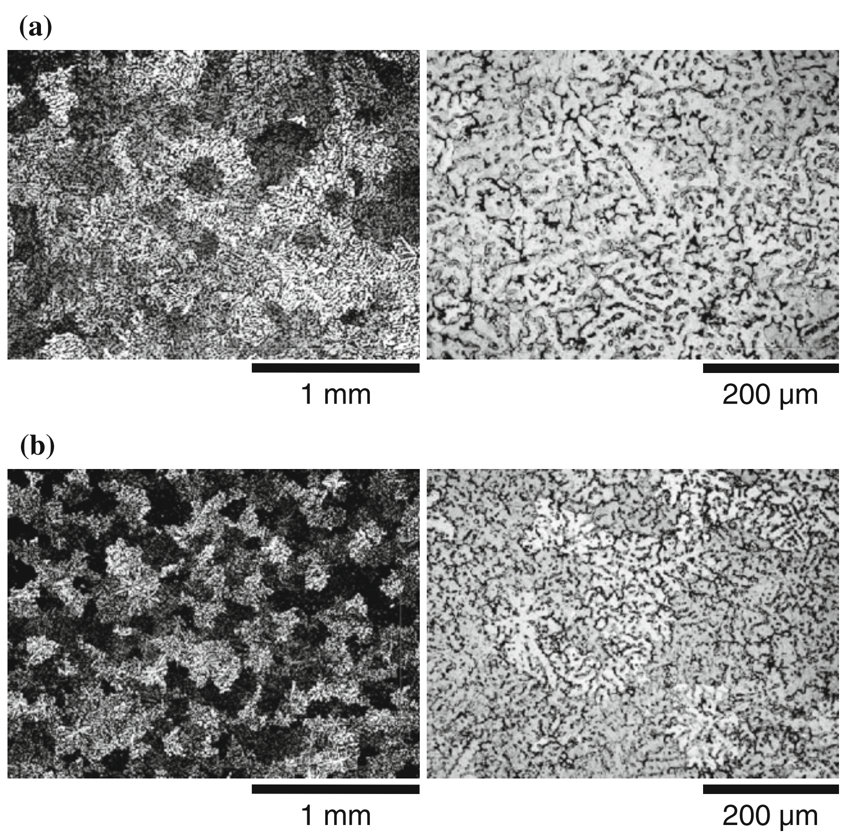

Fig. 1 **a** Coarse-microstructured (by direct chill billet casting) and **b** fine-microstructured (by adiabatic mold continuous casting) of AZX911 Mg alloys prepared by two casting methods

Table 1 Average grain size and dendrite arm spacing for cast AZX911 alloys

Casting method	Grain size (μm)	Dendrite arm spacing (μm)
Direct chill billet casting (coarse-microstructured)	290	26
Adiabatic mold continuous casting (fine-microstructured)	180	13

fine-microstructured samples, although the differences in the flow stresses were very small. These trends were also found in the s–s curves obtained from compression tests at 523 and 603 K.

Figure 3 shows the peripheral surfaces of the hot-forged samples. The coarse-microstructured samples suffered from edge crack formation during hot forging, regardless of the forging temperature and strain rate. However, the fine-microstructured samples exhibited smooth peripheral surfaces after hot forging at temperatures of 573 K and above. Although the fine-microstructured samples exhibited edge cracks after hot forging at 523 K, the opening widths of the cracks were much smaller than those in the coarse-microstructured samples hot forged at 523 K. These results demonstrate that the microstructural lengths, such as initial grain size and dendrite arm spacing, in the initial microstructure considerably affect the final surface quality of hot-forged Mg alloys. The finer the initial microstructure, the better the final quality of the free surface.

The microstructures of the coarse-microstructured and fine-microstructured samples after hot forging are shown in Figs. 4 and 5, respectively. Grain sizes were reduced to 2–5 μm by hot forging, as indicated by observations at a

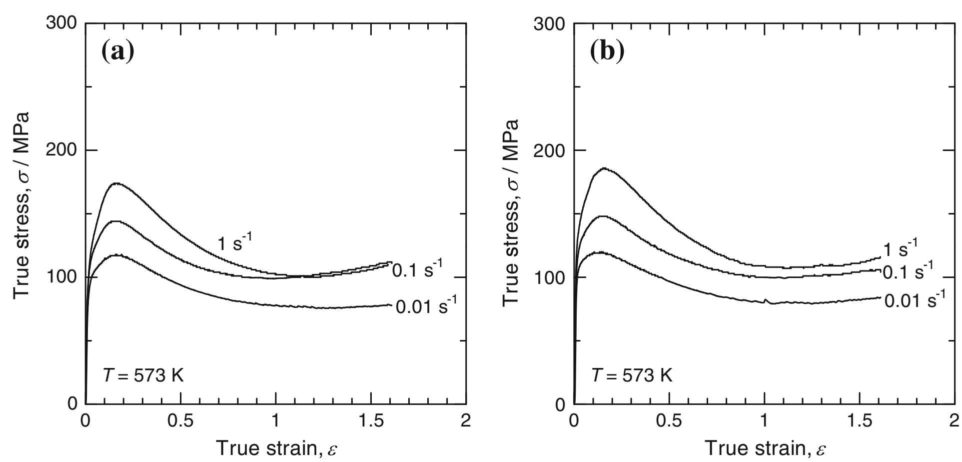

Fig. 2 True stress–strain curves obtained by compression tests at 573 K for (**a**) coarse- and (**b**) fine-microstructured AZX911 Mg alloys. Uniform deformation is assumed

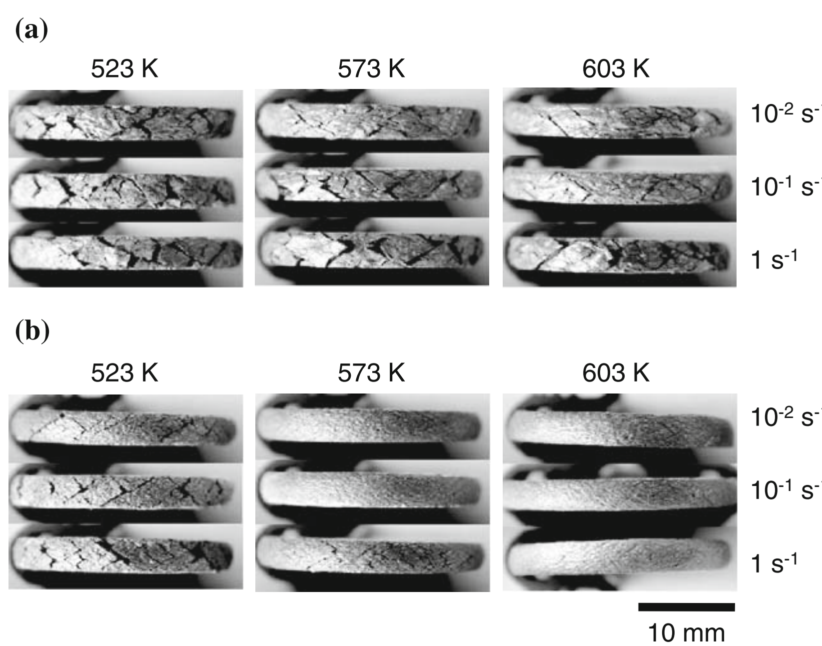

Fig. 3 Peripheral surfaces of (**a**) coarse- and (**b**) fine-microstructured AZX911 Mg alloy samples after hot compression to a true compressive strain of 1.6. The vertical axis shows compression direction

Fig. 4 Optical micrographs of coarse-microstructured AZX911 Mg alloy samples after hot compression to a true compressive strain of 1.6. The vertical axis shows compression direction. **a** Lower magnification, **b** higher magnification

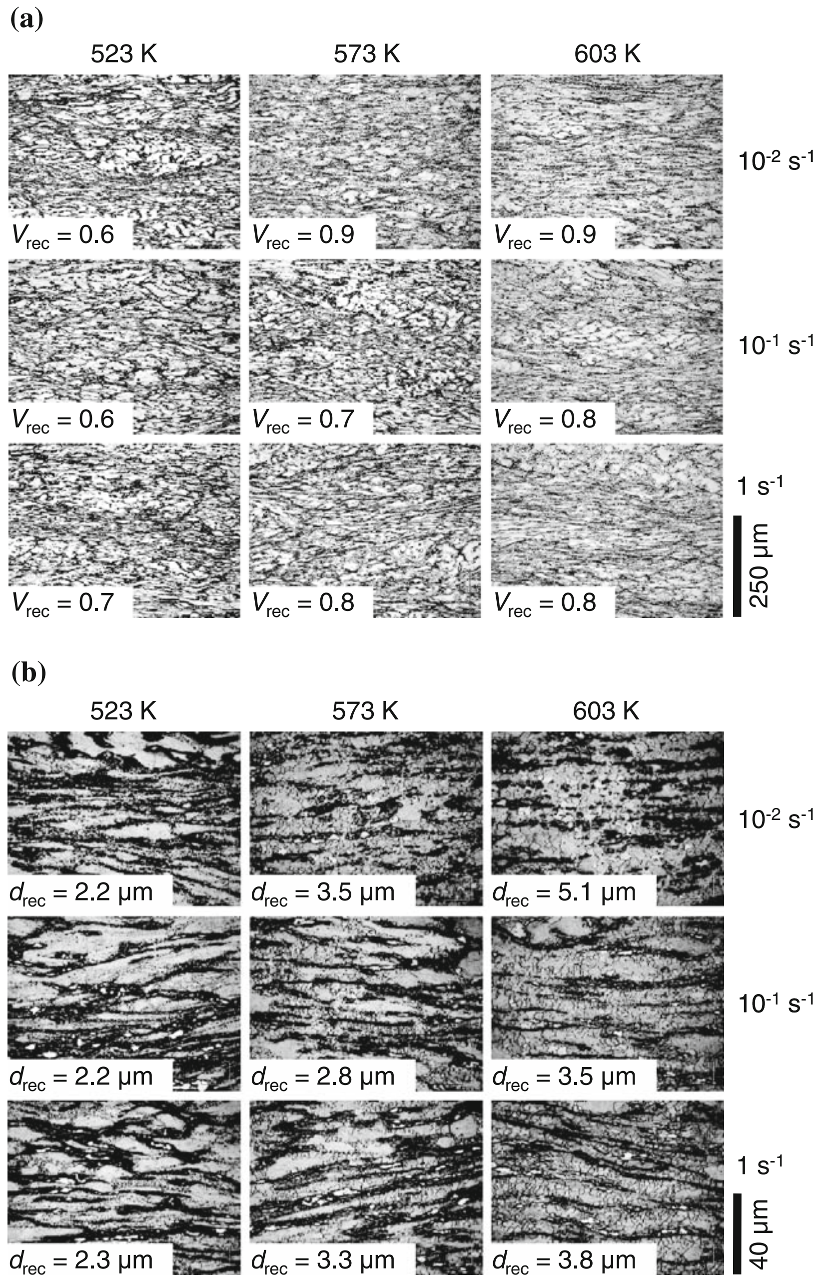

higher magnification. The reduction in grain size is due to DRX during hot forging. The recrystallized grains were localized around the second phases, which suggests that second phases as well as grain boundaries provide DRX sites [15–17]. The recrystallized grain size (d_{rec}) increased with the forging temperature; however, d_{rec} was less dependent on the strain rate. The fine-microstructured samples exhibited slightly smaller recrystallized grain sizes than the coarse-microstructured samples.

It has been reported that the recrystallized grain size depends on the initial grain size in the hot working of Mg alloys [20] and stainless steels [21, 22]. That is, a small initial grain size results in a small final recrystallized grain size after hot deformation. The dependence of d_{rec} on the length of initial microstructure (typically initial grain size) is often attributed to continuous DRX [4, 21, 22], which has a recrystallization mechanism different from that of conventional discontinuous DRX. It is difficult at this stage to judge whether continuous DRX is responsible for the present results. Electron backscattering diffraction analysis will be helpful for determining the DRX mechanism [21].

Watanabe et al. [20] correlated d_{rec} normalized by the initial grain size to the Zener–Hollomon parameter ($Z = \dot{\varepsilon}\exp(Q/RT)$), where $\dot{\varepsilon}$ is the strain rate, Q the activation energy for the dominant type of diffusion, R the gas constant, and T the absolute temperature. Figure 6 shows

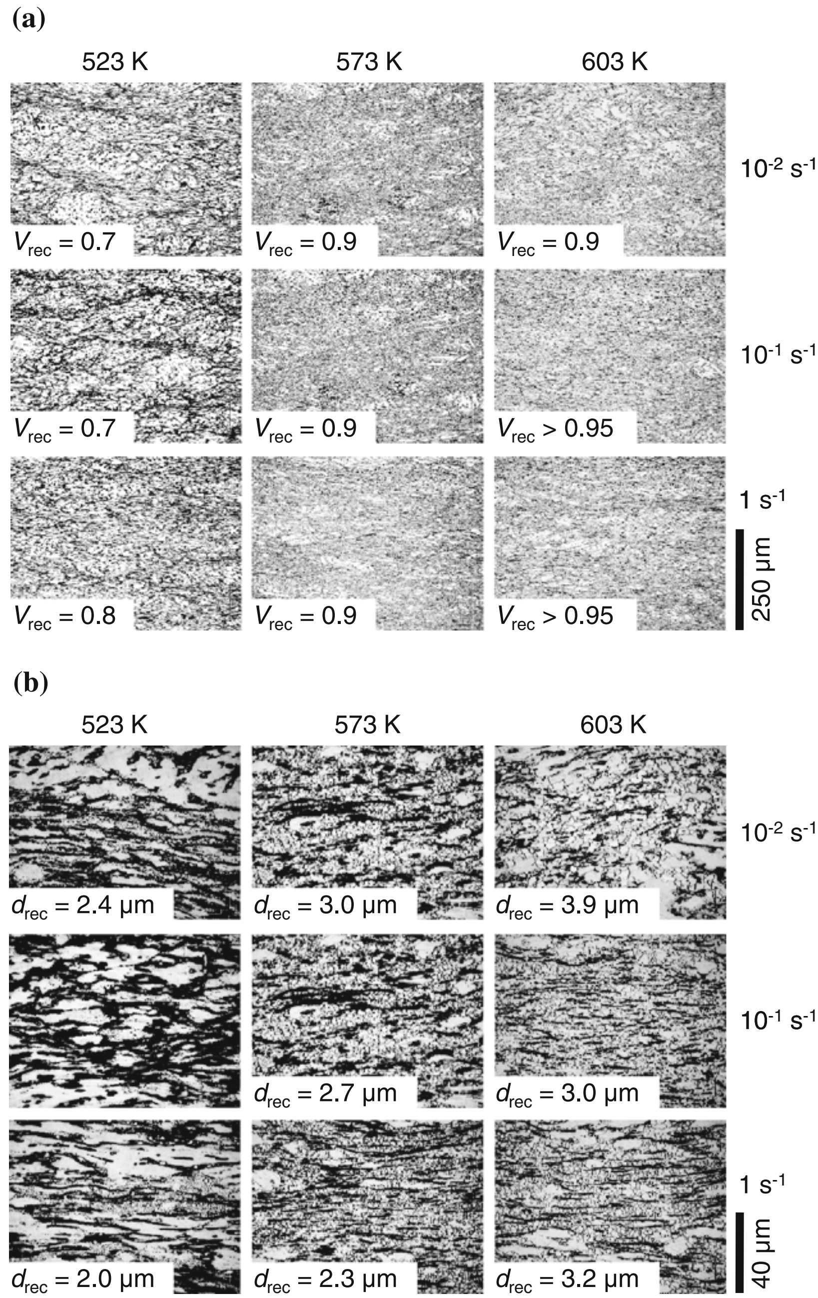

Fig. 5 Optical micrographs of fine-microstructured AZX911 Mg alloy samples after hot compression to a true compressive strain of 1.6. The vertical axis shows compression direction. **a** Lower magnification, **b** higher magnification

the relationship between Z and normalized d_{rec} for the present hot forging of AZX911, assuming that the dominant type of diffusion is lattice diffusion and $Q = 135$ kJ/mol [23]. In Fig. 6, d_{rec} is normalized by one of two microstructural lengths (d_0), that is, initial grain size or initial dendrite arm spacing. When d_0 is the initial grain size, d_{rec}/d_0 is much lower than that reported for AZ61 [20]; however, when d_0 is the initial dendrite arm spacing, d_{rec}/d_0 is comparable to that for AZ61 [20]. Therefore, the insoluble second phases between dendrites may serve as DRX-stimulating sites, as well as grain boundaries. The smaller slope of the d–Z plots for cast AZX911 than that for extruded AZ61 also indicates the effect of second phases on enhancing DRX [24], although a strict comparison between the present cast AZX911 Mg alloy and the extruded AZ61 Mg alloy in reference [20] may be meaningless.

The difference in d_{rec} between the two alloys is still too small to explain the difference in the peripheral surface after hot forging (Fig. 3). The recrystallized volume fraction (V_{rec}) was roughly estimated by analyses of the optical micrographs and shown in Figs. 4 and 5. V_{rec} was as high as 0.9–1 for the fine-microstructured samples hot forged at 573 and 603 K, which exhibited smooth peripheral

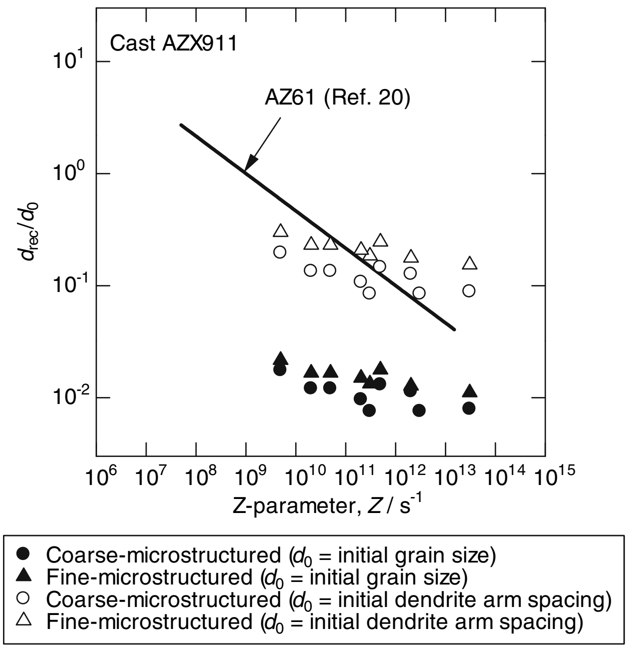

Fig. 6 Relationship between Zener–Hollomon parameter (Z) and recrystallized grain size (d_{rec}) normalized by initial grain size or initial dendrite arm spacing (d_0) for the present hot forging of AZX911 Mg alloys

surfaces; however, V_{rec} was 0.6–0.8 for almost all of the coarse-microstructured samples after hot forging, where the formation of edge cracks occurred. The finer dendritic microstructure appears to result in a larger V_{rec} by providing more DRX sites around the finely dispersed second phases. Considering the small difference in d_{rec} between the coarse-microstructured and fine-microstructured samples, it was found that the recrystallized volume fraction V_{rec}, rather than the recrystallized grain size d_{rec}, is closely related to the surface quality of forged Mg alloys. The size of the initial microstructure appears to be important for the successful hot forging of cast Mg alloys.

Conclusions

Two cast AZX911 alloys with coarse and fine initial microstructures were hot forged by compression tests at 523–603 K. The fine-microstructured AZX911 alloys exhibited a smooth peripheral surface when forged at 573 K and above, while the coarse-microstructured AZX911 alloys suffered from edge crack formation at all temperatures tested. The recrystallized volume fraction after hot forging was higher in the fine-microstructured AZX911 alloy, resulting in high free surface quality. The present results indicate that the reduction in dendrite arm spacing is important for uniform recrystallization because the second phases as well as grain boundaries provide sites for recrystallization.

Acknowledgement This study was conducted with the financial support of the Forged Magnesium Parts Technological Development Project, which is organized by New Energy and Industrial Technology Development Organization (NEDO), Japan.

References

1. Ebert T, Mordike BL (2001) Mater Sci Eng A 302:37
2. Chino Y, Mabuchi M, Shimojima K, Yamada Y, Wen C, Miwa K, Nakamura M, Asahina T, Higashi K, Aizawa T (2001) Mater Trans 42:414
3. Takigawa Y, Honda M, Uesugi T, Higashi K (2008) Mater Trans 49:1979
4. Yang X, Miura H, Sakai T (2003) Mater Trans 44:197
5. Ding H, Liu L, Kamado S, Ding W, Kojima Y (2007) Mater Sci Eng A 452–453:503
6. Helis L, Okayasu K, Fukutomi H (2006) Mater Sci Eng A 430:98
7. StJohn DH, Qian M, Easton MA, Cao P, Hildebrand Z (2005) Metall Mater Trans A 36:1669
8. Li M, Tamura T, Miwa K (2009) J Mater Res 24:145
9. Akiyama S, Ueno H, Sakamoto M, Hirai H, Kitahara A (2000) Materia Japan 39:72–74 (in Japanese)
10. Watanabe H, Yamaguchi M, Takigawa Y, Higashi K (2008) Mater Trans 49:1262
11. Watanabe H, Yamaguchi M, Takigawa Y, Higashi K (2007) Mater Sci Eng A 454–455:384
12. Chino Y, Jae-Seol L, Nakaura Y, Ohori K, Mabuchi M (2005) Mater Trans 46:2592
13. Chino Y, Nakaura Y, Ohori K, Kamiya A, Mabuchi M (2007) Mater Sci Eng A 452–453:31
14. Hakamada M, Watazu A, Saito N, Iwasaki H (2008) Mater Trans 49:554
15. Humphreys FJ (1991) Mater Sci Eng A 135:267
16. Hakamada M, Watazu A, Saito N, Iwasaki H (2008) Mater Trans 49:1032
17. Hakamada M, Watazu A, Saito N, Iwasaki H (2009) Mater Trans 50:711
18. Thompson AW (1972) Metallography 5:366
19. Barnett MR (2003) Mater Trans 44:571
20. Watanabe H, Tsutsui H, Mukai T, Ishikawa K, Okanda Y, Kohzu M, Higashi K (2001) Mater Trans 42:1200
21. Dehghan-Manshadi A, Hodgson PD (2008) Metall Mater Trans A 39:2830
22. Tsuzaki K, Huang X, Maki T (1996) Acta Mater 44:4491
23. Frost HJ, Ashby MF (1982) Deformation-mechanism maps. Pergamon Press, Oxford
24. Hakamada M, Watazu A, Saito N, Iwasaki H (2008) J Mater Sci 43:2066. doi:10.1007/s10853-008-2474-8